

# Fast-individual-harmonic-extraction technique

C.H. Ng, K. Busawon, G.A. Putrus and L. Ran

**Abstract:** Harmonic distortion in power networks is continuously increasing owing to the increased use of nonlinear loads in power-distribution networks. Consequently, harmonic monitoring and control are becoming particularly important for both utilities and consumers to reduce their harmful effects. In some applications, such as real-time harmonic monitoring and active filters, techniques for fast extraction of individual harmonic components are required. The relatively long response time of conventional techniques make them less appealing when the speed of response is important. The paper deals with the problem of individual-harmonic extraction for the purpose of harmonic filtering and compensation. A common problem associated with existing individual-harmonic-extraction techniques is the speed of extracting a single harmonic component, which determines the response of the compensator. Standard harmonic-extraction techniques are investigated and a new fast-individual-harmonic-extraction (FIHE) technique is proposed. It is shown that the proposed FIHE is capable of performing harmonic extraction six times faster than the Fourier transform and provides better filtering characteristics than traditional filters such as Butterworth and FIR filters. Computer simulation and laboratory experimental results are provided to illustrate the characteristics and performance of the proposed technique.

## 1 Introduction

Harmonic measurement is an important process when designing a harmonic filter or compensator. A power active filter works as a harmonic source, which reproduces the harmonic components of interest (synchronised to the harmonic components in the system) to achieve the desired compensation. In most cases, the desired harmonic components are reproduced by a power inverter, which constitutes the main part of the active filter. To obtain the reference signal for the inverter, it is necessary to extract the desired harmonic component(s) from the distorted current (or voltage) waveform in the system. In some applications, the fundamental component is removed from the signal detected and the remaining (nonfundamental) harmonic components are used to perform a total harmonic compensation (THC) [1, 2]. In certain applications, the active filter is only required to deal with selected dominant harmonic components of the distorted signal; this is known as individual harmonic compensation (IHC). Regardless of the use (THC or IHC), harmonic extraction is a necessary process which is required for obtaining the desired reference signal for the inverter. Most existing harmonic-extraction techniques are either based on filtering techniques in the time domain or Fourier analysis in the frequency domain.

In this paper the possibility of speeding up an individual harmonic extraction process is investigated. As a result, a fast-individual-harmonic-extraction (FIHE) technique is

proposed. It is shown that the FIHE is capable of performing harmonic-extraction six times faster than the Fourier transform and provides better filtering characteristics than traditional filters such as Butterworth and FIR filters. Computer simulation and laboratory experimental results are provided to illustrate the performance and characteristics of the proposed technique.

## 2 Harmonic extraction in time and frequency domains

In this section, standard methods of harmonic extraction in the time and frequency domains are analysed.

### 2.1 Harmonic extraction in the time domain

Harmonic extraction based on filtering can be divided largely into two methods [3]. The first method uses filters to extract selected harmonic components directly (phase by phase in a three-phase system). The second method makes use of the generalised Park transformation to convert the selected harmonic component from a 3-phase stationary reference frame to a synchronous reference frame and then perform harmonic extraction by using a simple lowpass filter [4, 5]. The most common filters are Butterworth, Chebyshev I/II, and Bessel types. Throughout this paper, discussion is restricted to the Butterworth-type lowpass filter; as it is generally acknowledged as a good 'all rounder' filter which gives a flat response in the passband and an adequate rate of roll-off.

The advantages of time-domain methods are that their design is straightforward and fewer computational steps are required; hence smaller processor memory is needed. The disadvantages are time delay, phase delay and gain/attenuation distortion.

To ensure synchronisation between the reproduced (by the active filter) and the system harmonic components, the active filter is required to be highly dynamic. As a result, it is desirable to have minimum delay in the process of regenerating harmonic components used for compensation.

© IEE, 2005

IEE Proceedings online no. 20045072

doi:10.1049/ip-gtd:20045072

Paper first received 15th June 2004 and in final revised form 22nd March 2005. Originally published online: 16th June 2005

C.H. Ng, K. Busawon and G.A. Putrus are with the School of Engineering, Northumbria University, Newcastle upon Tyne NE1 8ST, UK

L. Ran is with the School of Engineering, Durham University, Durham DH1 3LE, UK

E-mail: ghanim.putrus@unn.ac.uk

The inherent conflict between the frequency characteristics and time response of a filter forces a trade off between a good roll-off (better attenuation) and faster response. The higher the order of the filter the steeper is the roll-off in the frequency response and the better are the attenuation characteristics; but at the expense of a further delay in the response time. This phenomenon is demonstrated in Fig. 1 where the frequency response and the step response (time response) for Butterworth filters of different orders are shown.

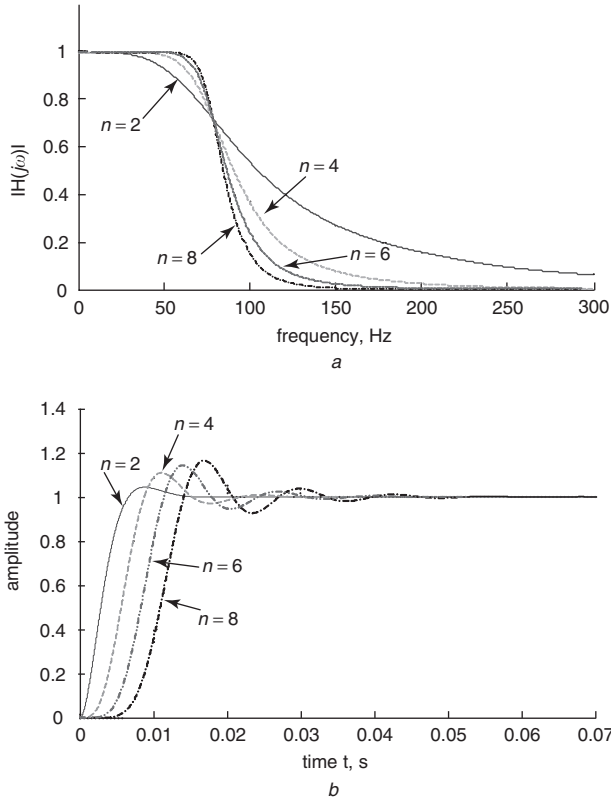


**Fig. 1** Frequency and step response for  $n$ th-order Butterworth lowpass filter  
 a Frequency response  
 b Step response

Generally, to permit extraction of the desired harmonic component, the attenuation of the filter must be sufficiently high in order to eliminate the unwanted harmonic components. This is not a problem in certain applications when only the fundamental component is required. As the ratio of harmonic quantities with respect to the fundamental component is very low, hence a low-attenuation (low-order) filter is enough to filter the harmonic components. However, in the case where one of the harmonic components is of interest (e.g.: fifth, seventh or, 11<sup>th</sup>), the harmonic magnitude is relatively low compared with the fundamental component. Therefore, a high-attenuation filter is required in order to eliminate all other components (i.e. first and fifth if seventh is of interest). This implies that a higher-order filter is required and hence longer time delay is to be expected.

For instance, to filter a seventh order harmonic voltage in a low-voltage system, where the fundamental voltage is 230 V, the seventh harmonic voltage is about 14% (33 V) of the fundamental voltage. As mentioned above, generalised Park transformation together with lowpass filters have been used to extract harmonics. Figure 2 demonstrates the effects of filter's order when a step function was applied to amplify the seventh-harmonic voltage at  $t = 50$  ms. The results show

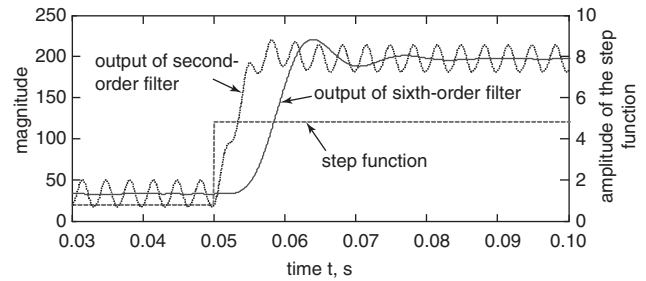


**Fig. 2** Effect of filter order

that some unwanted harmonic components remain in the filtered signal (as a ripple) when a second-order lowpass filter is used. When using a higher-order filter ( $n=6$ ), a smoother (ripple-less) output signal is produced, but the time response of the filter is slower.

In practice, in addition to the time delay introduced by a high-order filter, an increase in the order of the filter brings with it other problems, such as offset and noise error to the passband region. Moreover, a high-order filter often suffers from stability issues. It is familiar to most engineers that 'onboard tweaking' of capacitors, variable resistors etc. to avoid oscillation is always required for a high-order filter.

## 2.2 Frequency-domain harmonic extraction

Harmonic extraction in the frequency domain is based on Fourier analysis where information about the selected harmonic component(s) is used to reconstruct the signal in the time domain. Generally, the Fourier transform (FT) is used to convert a signal  $f(t)$  from the time domain to the frequency domain [6]. If  $f(t)$  is periodic with a period  $T_0$ , its Fourier transform (Fourier series) is given by

$$F(n\omega_0) = \frac{1}{T_0} \int_{t_0}^{t_0+T_0} f(t) \exp(-jn\omega_0 t) dt \quad (1)$$

where  $n=0, 1, 2, 3, \dots$  is the harmonic order, and  $\omega_0 = 2\pi/T_0$  is the frequency of the fundamental component (rad/s).

For individual harmonic extraction,  $n$  is the order of the required component (i.e.: 1st, 5th, 7th etc.).  $F(n\omega_0)$  contains the magnitude and phase information of the  $n$ th order component. The advantages of using the Fourier transform for individual harmonic extraction are that it gives a very good attenuation gain with no overshoot or oscillation problems. With these advantages, the FT provides an excellent extraction profile, as can be seen in the example shown in Fig. 4. However, the biggest disadvantage of using the FT is that, a minimum of one fundamental cycle is required for the transformation process. This is clearly shown in Fig. 3 and (1), where integration over a fundamental period ( $T_0$ ) is required. Therefore, in a 50 Hz system, 20 ms will be the minimum processing period for a harmonic component to be filtered.

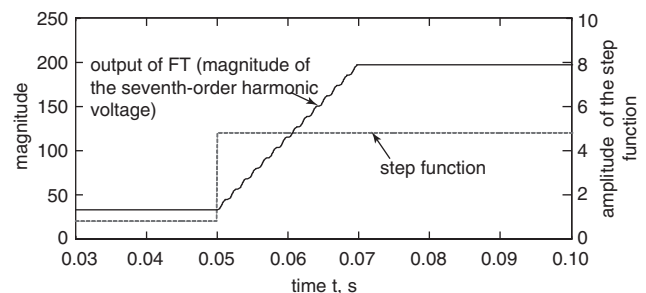


**Fig. 3** Time response of the Fourier transformation

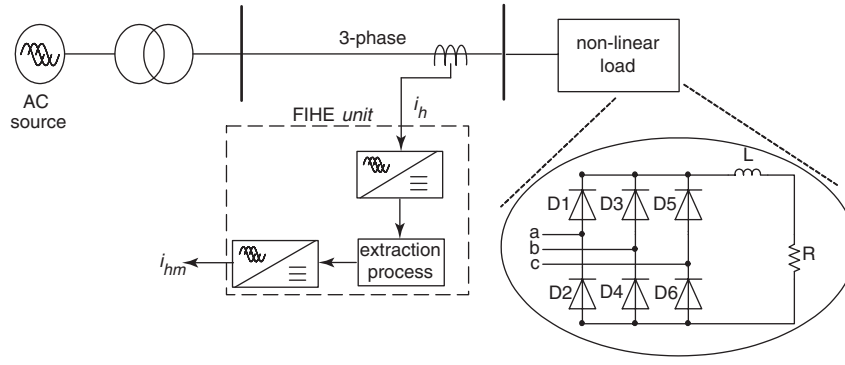


Fig. 4 System used in the simulation

### 3 Fast-individual-harmonic-extraction (FIHE) technique

In this Section, the fast-individual-harmonic-extraction method is presented following some preliminary observations. As will become clear in this paper, the proposed method is intended for harmonics that are balanced between the three phases. This is more usual in industrial power systems such as those found in the steel industry and on offshore oil rigs where the harmonics are predominantly caused by large motor drives. Unbalance and noncharacteristic harmonics may exist in some utility distribution systems comprising considerable single-phase loads. The performance of the proposed method will decrease depending on the degree of unbalance.

In the analyses below, note that the set of natural numbers is denoted by  $N$ , the set of positive odd numbers by  $2N+1$  and the set of positive even numbers by  $E$ .

#### 3.1 Preliminary observations

Consider the following balanced three-phase signal containing harmonics of the order  $n \in 2N+1$ :

$$S_{ABC}(t, n) = \begin{bmatrix} S_A(t, n) \\ S_B(t, n) \\ S_C(t, n) \end{bmatrix} = \begin{bmatrix} M_n \cos(n\omega_0 t) \\ M_n \cos\left(n\omega_0 t - \frac{2\pi n}{3}\right) \\ M_n \cos\left(n\omega_0 t + \frac{2\pi n}{3}\right) \end{bmatrix} \quad (2)$$

The signal  $S_{ABC}(t, n)$  can be converted to a single-phase signal by using the conversion function

$$\Gamma_d(t, m) = \begin{bmatrix} \sin(m\omega_0 t) & \sin\left(m\omega_0 t - \frac{2\pi n}{3}\right) & \sin\left(m\omega_0 t + \frac{2\pi n}{3}\right) \end{bmatrix} \quad (3)$$

where  $m \in 2N+1$ .

The resultant converted single-phase signal is given by

$$\begin{aligned} \beta(t, m, n) &= \frac{2}{3} \Gamma_d(t, m) S_{ABC}(t, n) \\ &= \frac{2}{3} M_n \sin(m\omega_0 t) \sin(n\omega_0 t) \\ &+ \frac{2}{3} M_n \sin\left(m\omega_0 t - \frac{2\pi n}{3}\right) \sin\left(n\omega_0 t - \frac{2\pi n}{3}\right) \\ &+ \frac{2}{3} M_n \sin\left(m\omega_0 t + \frac{2\pi n}{3}\right) \sin\left(n\omega_0 t + \frac{2\pi n}{3}\right) \end{aligned} \quad (4)$$

Since  $\sin(a) \sin(b) = \frac{1}{2} \{\cos(a-b) - \cos(a+b)\}$

$$\begin{aligned} \beta(t, m, n) &= \frac{1}{3} M_n [\cos\{(m-n)\omega_0 t\} - \cos\{(m+n)\omega_0 t\}] \\ &+ \frac{1}{3} M_n \left[ \cos\left\{(m-n)\omega_0 t - \frac{2}{3}\pi(m-n)\right\} \right. \\ &- \cos\left\{(m+n)\omega_0 t - \frac{2}{3}\pi(m+n)\right\} \left. \right] \\ &+ \frac{1}{3} M_n \left[ \cos\left\{(m-n)\omega_0 t + \frac{2}{3}\pi(m-n)\right\} \right. \\ &- \cos\left\{(m+n)\omega_0 t + \frac{2}{3}\pi(m+n)\right\} \left. \right] \end{aligned} \quad (5)$$

Depending on the values of  $n$  and  $m$ , the value of  $\beta(t, m, n)$  can either be zero or nonzero. To have a better and clear insight of the values of  $\beta(t, m, n)$ , consider the three sequences  $\{u_k\}$ ,  $\{v_k\}$ ,  $\{w_k\}$ ; ( $k=0, 1, 2, \dots$ ) defined as:

$$\begin{aligned} u_k &= 3k \\ v_k &= 3k+1 \\ w_k &= 3k+2 \end{aligned} \quad (6)$$

Let

$$\begin{aligned} U &= \cup \{u_k\} |_{k=0,1,2,\dots} \\ V &= \cup \{v_k\} |_{k=0,1,2,\dots} \\ W &= \cup \{w_k\} |_{k=0,1,2,\dots} \end{aligned}$$

It can readily be seen that the sets  $U$ ,  $V$  and  $W$  form a partition of the set of natural numbers  $N$ , i.e.

$$N = U \cup V \cup W$$

As mentioned above, both  $n$  and  $m$  are positive odd numbers. Consequently, the terms  $|m-n|$  or  $|m+n|$  stated in (5) are even. Therefore, it is easier to explain and understand the algorithm of the proposed technique in the even-number domain. For the sequences described in (6), the set of positive even numbers  $E$  can be partitioned into three disjoint sets,  $X$ ,  $Y$  and  $Z$ , defined as:

$$\begin{aligned} X &= \cup \{x_k\} |_{k=0,1,2,\dots} \\ Y &= \cup \{y_k\} |_{k=0,1,2,\dots} \\ Z &= \cup \{z_k\} |_{k=0,1,2,\dots} \end{aligned} \quad (7)$$

where the sequences  $\{x_k\}$ ,  $\{y_k\}$ ,  $\{z_k\}$ ; ( $k=0, 1, 2, \dots$ ) are defined by:

$$\begin{aligned} x_k &= 2u_k = 6k \\ y_k &= 2v_k = 6k+2 \\ z_k &= 2w_k = 6k+4 \end{aligned}$$

Note that for every number  $u_k \in U$ ,  $v_k \in V$  and  $w_k \in W$ :

$$\frac{2\pi}{3}(u_k) = \frac{2\pi}{3}(3k) = 2\pi = 0^\circ \quad (\text{zero-sequence}) \quad (8)$$

$$\begin{aligned} \frac{2\pi}{3}(v_k) &= \frac{2\pi}{3}(3k+1) = 2\pi + \frac{2\pi}{3} \\ &= 120^\circ \quad (\text{positive-sequence}) \end{aligned} \quad (9)$$

$$\begin{aligned} \frac{2\pi}{3}(w_k) &= \frac{2\pi}{3}(3k+2) = 2\pi + \frac{4\pi}{3} \\ &= -120^\circ \quad (\text{negative-sequence}) \end{aligned} \quad (10)$$

Equations (8), (9) and (10) show that, irrespective of the harmonic order in  $U$  (3rd, 9th, 15th etc.), there will always be a zero-sequence component. Also, whichever harmonic order is found in  $V$  (1st, 7th, 13th etc.), this will result in a positive-sequence component. Similarly, the harmonic order in  $W$  (2nd, 5th, 11th etc.) will result in a negative-sequence component. This also happen in the even-number domain, for every number  $x_k \in X$ ,  $y_k \in Y$  and  $z_k \in Z$ . Therefore,

$$\frac{2\pi}{3}(x_k) = \frac{2\pi}{3}(6k) = 4\pi = 0^\circ \quad (\text{zero-sequence}) \quad (11)$$

$$\begin{aligned} \frac{2\pi}{3}(y_k) &= \frac{4\pi}{3}(3k+1) = 4\pi + \frac{4\pi}{3} \\ &= -120^\circ \quad (\text{negative-sequence}) \end{aligned} \quad (12)$$

$$\begin{aligned} \frac{2\pi}{3}(z_k) &= \frac{4\pi}{3}(3k+2) = 4\pi + \frac{8\pi}{3} \\ &= 120^\circ \quad (\text{positive-sequence}) \end{aligned} \quad (13)$$

In the following, both  $m$  and  $n$  are positive and odd, so that  $|n-m|$  and  $|m+n|$  are both even.

To determine the value of  $\beta(t, m, n)$ , there are nine cases to be considered:

Case 1:  $|m-n| \in X$  and  $|m+n| \in X$

$$\begin{aligned} \beta(t, m, n) &= \frac{1}{3}M_n[\cos\{(m-n)\omega_0 t\} - \cos\{(m+n)\omega_0 t\}] \\ &\quad + \frac{1}{3}M_n[\cos\{(m-n)\omega_0 t\} - \cos\{(m+n)\omega_0 t\}] \\ &\quad + \frac{1}{3}M_n[\cos\{(m-n)\omega_0 t\} - \cos\{(m+n)\omega_0 t\}] \\ &= M_n \cos\{(m-n)\omega_0 t\} - M_n \cos\{(m+n)\omega_0 t\} \end{aligned} \quad (14)$$

Case 2:  $|m-n| \in X$  and  $|m+n| \in Y$

$$\begin{aligned} \beta(t, m, n) &= \frac{1}{3}M_n[\cos\{(m-n)\omega_0 t\} - \cos\{(m+n)\omega_0 t\}] \\ &\quad + \frac{1}{3}M_n \left[ \cos\{(m-n)\omega_0 t\} \right. \\ &\quad \left. - \cos\left\{(m+n)\omega_0 t + \frac{2}{3}\pi\right\} \right] \\ &\quad + \frac{1}{3}M_n \left[ \cos\{(m-n)\omega_0 t\} \right. \\ &\quad \left. - \cos\left\{(m+n)\omega_0 t - \frac{2}{3}\pi\right\} \right] \\ &= M_n \cos\{(m-n)\omega_0 t\} \end{aligned} \quad (15)$$

Similarly, the values of  $\beta(t, m, n)$  in the following cases can be verified:

Case 3:  $|m-n| \in X$  and  $|m+n| \in Z$

$$\beta(t, m, n) = M_n \cos\{(m-n)\omega_0 t\}$$

Case 4:  $|m-n| \in Y$  and  $|m+n| \in X$

$$\beta(t, m, n) = -M_n \cos\{(m+n)\omega_0 t\}$$

Case 5:  $|m-n| \in Y$  and  $|m+n| \in Y$

$$\beta(t, m, n) = 0$$

Case 6:  $|m-n| \in Y$  and  $|m+n| \in Z$

$$\beta(t, m, n) = 0$$

Case 7:  $|m-n| \in Z$  and  $|m+n| \in X$

$$\beta(t, m, n) = -M_n \cos\{(m+n)\omega_0 t\}$$

Case 8:  $|m-n| \in Z$  and  $|m+n| \in Y$

$$\beta(t, m, n) = 0$$

Case 9:  $|m-n| \in Z$  and  $|m+n| \in Z$

$$\beta(t, m, n) = 0$$

### 3.2 Application of the FIHE to a 50 Hz system

For a three-phase balanced 50 Hz system, only five of these cases are relevant; these are: cases 1, 2, 3, 4 and 7. The relevant nonzero cases are summarised in Table 1.

Table 1: Nonzero Cases

Case	$ m-n $	$ m+n $	$\beta$
1	X	X	$M_n \cos\{(m-n)\omega_0 t\} - M_n \cos\{(m+n)\omega_0 t\}$
2	X	Y	$M_n \cos\{(m-n)\omega_0 t\}$
3	X	Z	$M_n \cos\{(m-n)\omega_0 t\}$
4	Y	X	$-M_n \cos\{(m+n)\omega_0 t\}$
7	Z	X	$-M_n \cos\{(m+n)\omega_0 t\}$

Note that, when  $|m-n| \in X$  (for cases 2 and 3),  $\beta(t, m, n) = M_n \cos(6k\omega_0 t)$ .

Similarly, when  $|m+n| \in X$  (for cases 4 and 7),  $\beta(t, m, n) = -M_n \cos(6k\omega_0 t)$ .

Finally, when both  $|m-n| \in X$  and  $|m+n| \in X$  (for case 1),

$$\beta(t, m, n) = M_n \cos(6k\omega_0 t) - M_n \cos(6k\omega_0 t)$$

This means that the smallest frequency component that appears in  $\beta(t, m, n)$  is always  $6\omega_0 = 6 \times 2\pi \times 50$  rad/s or 300 Hz.

Let

$$\tau_6 = \frac{T_0}{6} = \frac{1}{6 \times 50} = \frac{1}{300} \text{ seconds}$$

Also, since  $n$  is odd and positive and assuming  $n = 2p + 1$  with  $p \in \mathbb{N}$ , it is clear that:

$$I_d(m) = \frac{1}{T_0} \int_{T_0}^{+\infty} \sum_{p=0}^{+\infty} \beta(m, 2p+1, t) dt \quad (16)$$

$$\begin{aligned} &= \frac{1}{\tau_6} \int_{\tau_6}^{+\infty} \sum_{p=0}^{+\infty} \beta(m, 2p+1, t) dt \\ &= \begin{cases} 0 & \text{if } n = 2p+1 \neq m \\ M_m & \text{if } n = 2p+1 = m \end{cases} \end{aligned} \quad (17)$$

where the closed interval of length  $T_0$  is denoted by  $T_0 = [t_0, t_0 + T_0]$  with  $t_0$  being a real number. More specifically,  $\int_{T_0} f(t) dt = \int_{t_0}^{t_0+T_0} f(t) dt$ .

This means that there is no need to integrate  $\beta(m, n, t)$  over the full period  $T_0$  to obtain  $I(m)$ ; an integration over a period of one-sixth of  $T_0$  is sufficient. This last observation forms the basis of the FIHE method. In this method, it is clear that, the time taken to extract the harmonic

component is six times faster than the original method. Further, as will be shown, the proposed FIHE scheme has the advantages of being overshoot-free, oscillation-free and it has high attenuation gain characteristics, which cannot be found in existing filtering technique.

### 3.3 Reconstruction of the extracted harmonic signal

As explained in Section 3.2, a harmonic component can be extracted and expressed in a DC form as  $I(m)$ . However, in some applications, the time-domain waveform of the harmonic is important and needs to be available after extraction; hence a bidirectional transformation is required. Therefore, to reconstruct the extracted harmonic signal, an equal weight matrix is required which means that two extra sets of variables are needed:  $\gamma(m, n, t)$  and  $\delta(m, n, t)$ . For simplicity and to provide all phase information,  $\gamma(m, n, t)$  has to be set perpendicular to the first set of variables  $\beta(m, n, t)$ ; i.e.

$$\gamma(m, n, t) = \frac{2}{3} \Gamma_q(t, m) S_{ABC}(t, n) \quad (18)$$

where

$$\Gamma_q(t, m) = \left\{ \begin{array}{ccc} \cos(m\omega_0 t) & \cos\left(m\omega_0 t - \frac{2\pi m}{3}\right) & \cos\left(m\omega_0 t + \frac{2\pi m}{3}\right) \end{array} \right\} \quad (19)$$

Using the previous analysis, it can be noted that the smallest frequency component that appears in  $\gamma(m, n, t)$  is also  $6\omega_0$ . On the other hand, since  $\int_{T_0} \sin(m\omega_0 t) \cos(n\omega_0 t) dt = 0$ , for all  $n$  and  $m$ , this results in

$$I_q(m) = \frac{1}{T_0} \int_{T_0} \sum_{p=0}^{+\infty} \gamma(m, 2p+1, t) dt \quad (20)$$

$$= \frac{1}{\tau_6} \int_{\tau_6} \sum_{p=0}^{+\infty} \gamma(m, 2p+1, t) dt = 0 \quad (21)$$

Finally,  $\delta(m, n, t)$  is defined by

$$\delta(m, n, t) = \frac{2}{3} \Gamma_0(t, m) S_{ABC}(t, n) \quad (22)$$

where

$$\Gamma_0 = \begin{bmatrix} 1 & 1 & 1 \\ 2 & 2 & 2 \end{bmatrix} \quad (23)$$

It is clear that  $\gamma(m, n, t) = 0$  and  $\delta(m, n, t) = 0$ , since  $S_{ABC}(t, n)$  is a balanced three-phase signal. Consequently,

$$I_0(m) = \frac{1}{\tau_6} \int_{\tau_6} \sum_{p=0}^{+\infty} \delta(m, 2p+1, t) dt = 0 \quad (24)$$

Equations (4), (18) and (22) can be written in compact form as

$$\Psi(m, n, t) = \frac{2}{3} \Gamma(t, m) S_{ABC}(t, n) \quad (25)$$

where

$$\Psi(m, n, t) = \begin{bmatrix} \beta(m, n, t) \\ \gamma(m, n, t) \\ \delta(m, n, t) \end{bmatrix} \quad (26)$$

and

$$\Gamma(t, m) = \begin{bmatrix} \sin(m\omega_0 t) & \sin\left(m\omega_0 t - \frac{2\pi m}{3}\right) & \sin\left(m\omega_0 t + \frac{2\pi m}{3}\right) \\ \cos(m\omega_0 t) & \cos\left(m\omega_0 t - \frac{2\pi m}{3}\right) & \cos\left(m\omega_0 t + \frac{2\pi m}{3}\right) \\ \frac{1}{2} & \frac{1}{2} & \frac{1}{2} \end{bmatrix} \quad (27)$$

Finally,  $I(m)$  can be obtained as:

$$I(m) = \frac{1}{\tau_6} \int_{\tau_6} \sum_{p=0}^{+\infty} \Psi(m, 2p+1, t) dt \quad (28)$$

To reconstruct the signal  $S_{abc}(t, m)$  the following equation is applied:

$$S_{abc}(t, m) = \Gamma^{-1}(t, m) I(m) \quad (29)$$

where  $\Gamma^{-1}(t, m)$  is the reverse of  $\Gamma(t, m)$  and

$$I(m) = \begin{bmatrix} I_d(m) \\ I_q(m) \\ I_0(m) \end{bmatrix} \quad (30)$$

## 4 Evaluation of the proposed FIHE technique

Performance of the proposed harmonic-extraction technique is evaluated by using a computer simulation based on a typical 400 V three-phase supply system with a three-phase diode-bridge rectifier (with a 31 kW  $R$ - $L$  load) acting as a harmonic current source. The circuit configuration is shown in Fig. 4.

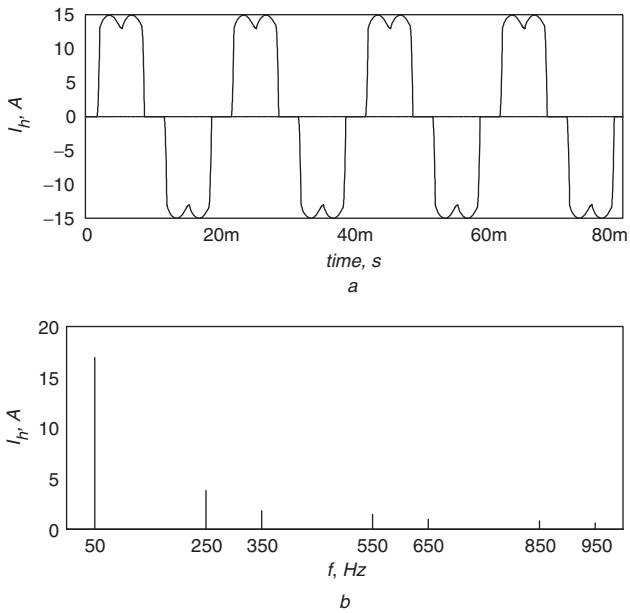
Simulation work was carried out in the Ansoft Simplorer environment [7, 8]. The harmonic current  $i_h$  produced by the nonlinear load was detected at the mains input feeder. The current  $i_h$  is fed to the proposed FIHE unit to extract the selected harmonic current  $i_{hm}$ . The extracted harmonic current  $i_{hm}$  is then converted back to a sinusoidal form. Figure 5 shows the waveform of the extracted current  $i_h$  together with its harmonic spectrum.

Figure 6 shows an example of the extracted seventh-order harmonic-current waveform where the detected current (given in Fig. 5) is shown in the background. The harmonic spectrum shown in Fig. 6b demonstrates that only the seventh-harmonic component exists after extraction.

The above results demonstrate the steady-state harmonic extraction-capability of the proposed FIHE technique. However, the most important feature of FIHE is its good dynamic characteristic. Therefore, dynamic-response tests were carried out in both computer simulation and laboratory experiments. A waveform with harmonic content up to 11th-order has been artificially created for the test. A step function for the seventh-harmonic component has been added into the waveform, which step up the seventh-harmonic component by five times the original value at  $t = 0.03$  s. The resultant waveform and the step function are shown in Fig. 7.

The signal shown in Fig. 7b was fed to the FIHE unit and the FIHE performance is shown in Fig. 8. The signal  $I(m)$  of the FIHE is shown in Fig. 8a and the extracted signal is shown in Fig. 8b. These results demonstrate that the proposed FIHE has a very fast (dynamic) response and provides zero overshoot as well as an oscillation-free characteristic. For comparison, Fig. 9 shows the response obtained when using standard harmonic-extraction techniques, i.e. lowpass filter and Fourier transform) and the





**Fig. 5** Waveform and frequency response of the extracted system current  $i_h$   
*a* Current  
*b* Frequency spectrum

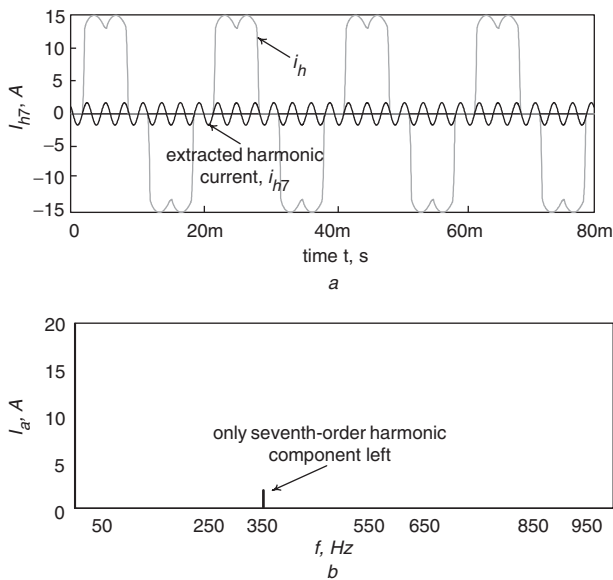


**Fig. 6** Waveform and frequency response of the extracted seventh-harmonic current  
*a* Extracted seventh-harmonic current and  $i_h$  waveform  
*b* Frequency response of seventh-harmonic current

proposed FIHE technique. These results show the good performance of the FIHE technique compared with that of the standard harmonic-extraction techniques.

Laboratory experimental work was conducted with the same scenario described above. Figure 10*a* shows the step-function signal and the signal  $I(m)$  of the FIHE with the step function. Figure 10*b* shows the signal  $I(m)$ , the distorted input signal, and the extracted seventh-harmonic signal (with the step function added). The results shown demonstrate clearly the functionality and accuracy of the proposed FIHE technique.

The proposed method is applicable to both odd and even harmonics. It has been noted that the accuracy of the FIHE technique drops when extracting harmonic components

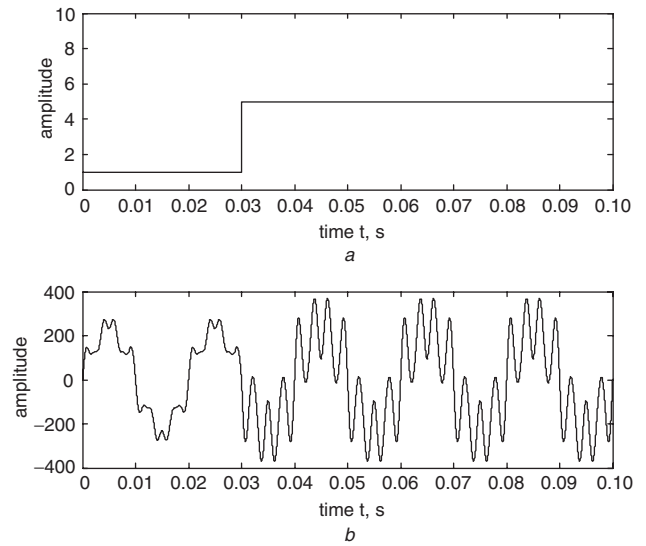


**Fig. 7** Waveform generated with the step function added  
*a* Step function for seventh-harmonic  
*b* Resultant waveform

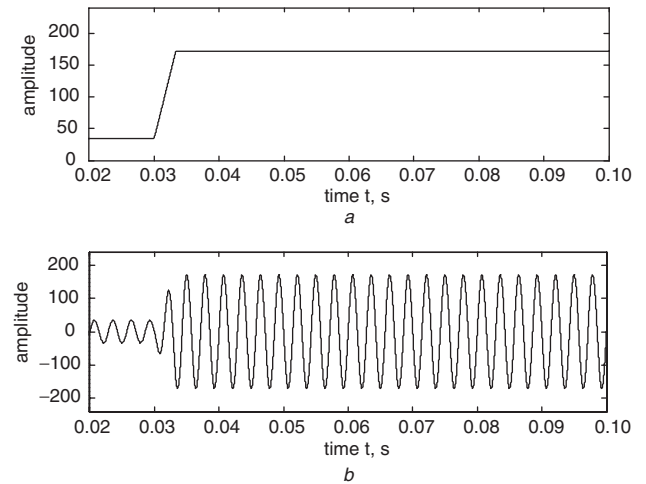


**Fig. 8** FIHE performance for a step change in the seventh-harmonic component  
*a*  $I_d(m)$  of the FIHE  
*b* Extracted seventh-harmonic component (perphase)

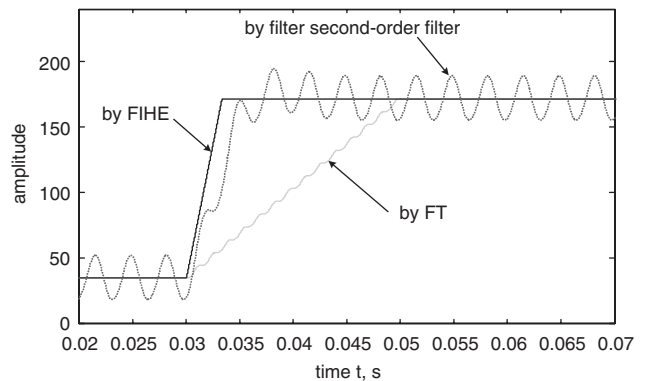


**Fig. 9** Time-response plot of three different harmonic-extraction techniques

from a three-phase signal that is unbalanced. For the system shown in Fig. 4, unbalance in the supply voltage will cause noncharacteristic harmonics in the system. Initial investigation indicates that, for a moderate supply unbalance, the

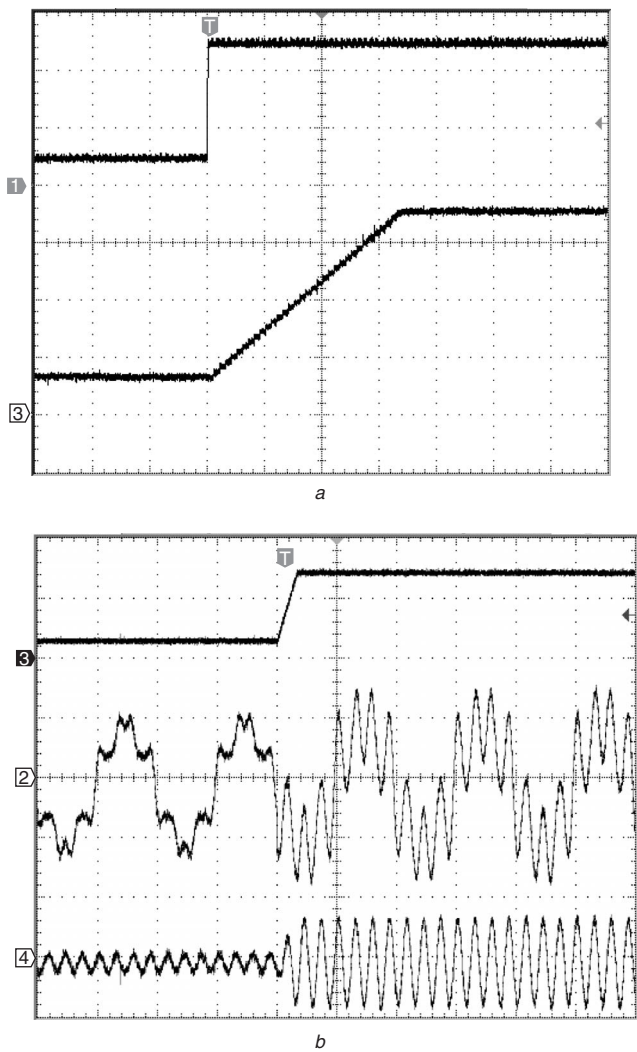


**Fig. 10** Experimental results

*a* The step signal and  $I(m)$  signal of the FIHE  
 Channel 1: Step-function signal (V): 2 V/division  
 Channel 2:  $I(m)$  of FIHE (V): 0.2 V/division

*b*  $I(m)$  signal, distorted signal, and the extracted seventh-harmonic component

Time: 10 ms/division

Channel 3:  $I(m)$  of FIHE (V): 0.2 V/division

Channel 2: Distorted signal (V): 1 V/division

Channel 4: Extracted seventh-harmonic component (V): 1 V/division

error introduced into the extracted harmonics of each phase is in the range 3–6%. If the harmonics in the three phases are unbalanced due to, for example, single-phase nonlinear loads, the proposed method will derive the same harmonic level for all three phases and the error introduced will be proportional to the degree of unbalance. A more thorough investigation is underway to quantify these errors.

## 5 Conclusions

This paper presents the principles, characteristics and performance of a new fast-individual-harmonic-extraction (FIHE) technique. The principles of the proposed technique and its performance are compared with existing standard harmonic-extraction techniques. The FIHE technique has an excellent dynamic-response capability (six times faster than standard techniques, e.g. the Fourier transform) and provides overshoot-free and ripple-free characteristics. The results obtained from the computer simulation and laboratory experimental work show a very high degree of confidence in the proposed technique.

The good dynamic performance of the proposed technique makes it an excellent tool when the speed of response is important, as in modern harmonic-control techniques such as, active power-harmonic compensators.

## 6 References

- 1 Peng, F.Z., Akagi, H., and Nabae, A.: 'A new approach to harmonic compensation in power systems'. Industry Applications Society Annual Meeting, Pittsburg, USA, 1988, Vol. 1, pp. 874–880
- 2 Akagi, H., Fujita, H., and Wada, K.: 'A shunt active filter based on voltage detection for harmonic termination of a radial power distribution line'. *IEEE Trans.*, 1999, **IA-35**, pp. 638–645
- 3 Tan, P.C., Holmes, D.G., and Morrison, R.E.: 'Control of active filter in the 25 kV AC traction systems'. Power Electronic Publication in AUPEC, 2000
- 4 Tnani, S., Mazaudier, M., Berthon, A., and Diop, S.: 'Comparison between different real-time harmonic analysis methods for control of electrical machines'. Power Electronics and Variable-Speed Drives, IEE Conf. Publ. 399, London, 1994
- 5 Ng, C.H., Ran, L., Putrus, G.A., and Busawon, K.: 'A new approach to real time individual harmonic extraction'. IEEE Power Electron. and Drive Systems Conference, Singapore, 2003
- 6 Vladimir, A.K.: 'Computer based harmonic measurement systems: discussion and a realization'. ICHPS V Int. Conf., Atlanta, USA, Sep. 1992, pp. 16–22
- 7 Ansoft, Co.: 'Simplorer v 6.0 multi domain simulation package user manual' (Ansoft Corporation, 2002) English ed
- 8 <http://www.ansoft.com/products/em/simplorer/> accessed in Feb 2004